JOURNAL OF VIROLOGY, Oct. 2009, p. 10605–10615 Vol. 83, No. 20
0022-538X/09/$08.00+0 doi:10.1128/JVI.01090-09

Respiratory Syncytial Virus Infection Induces a Reactive Oxygen Species–MSK1–Phospho-Ser-276 RelA Pathway Required for Cytokine Expression▽

Mohammad Jamaluddin,[1] Bing Tian,[2] Istvan Boldogh,[3] Roberto P. Garofalo,[4] and Allan R. Brasier[1,2]*

Institute for Translational Sciences[1] and Departments of Medicine,[2] Microbiology and Immunology,[3] and Pediatrics,[4] University of Texas Medical Branch (UTMB), Galveston, Texas 77555-1060

Received 28 May 2009/Accepted 4 August 2009

Respiratory syncytial virus (RSV) is a human pathogen that induces airway inflammation, at least in part, by modulating gene expression programs in airway epithelial cells. The presence of RSV replication is detected by the intracellular retinoic acid-inducible gene I (RIG-I) RNA helicase that forms a productive signaling complex with the mitochondrion-anchored MAVS protein, resulting in nuclear translocation of the NF-κB transcription factor. Although nuclear translocation is a prerequisite for activation of the innate inflammatory response, recent studies show that separate pathways governing RelA activation are also required for target gene expression. In this study, we examine the mechanism of RelA phosphorylation and its requirement for RSV-induced gene expression. RSV infection produced a time-dependent RelA phosphorylation on serine (Ser) residues Ser-276 and Ser-536 in parallel with enhanced reactive oxygen species (ROS) stress. Inhibition of RSV-induced ROS inhibited formation of phospho-Ser-276 RelA without affecting phospho-Ser-536 RelA formation. RSV potently induced activation of cytoplasmic mitogen- and stress-related kinase 1 (MSK1) in an ROS-dependent manner. Inhibition of MSK1 using H89 and small interfering RNA knockdown both reduced RSV-induced phospho-Ser-276 RelA formation and expression of a subset of NF-κB-dependent genes. Direct examination of the role of phospho-Ser-276 in target gene expression by expression of a RelA Ser-276-to-Ala site mutation in RelA$^{-/-}$ mouse embryonic fibroblasts showed that the mutation was unable to mediate RSV-induced NF-κB-dependent gene expression. We conclude that RSV induces RelA activation in the innate inflammatory response via a pathway separate from that controlling RelA cytoplasmic release, mediated by ROS signaling to cytoplasmic MSK1 activation and RelA Ser-276 phosphorylation.

Respiratory syncytial virus (RSV) is a major human pathogen responsible for epidemic bronchiolitis, exacerbation of respiratory dysfunction in children with bronchodysplasia, cystic fibrosis, and nosocomial outbreaks in the elderly (5, 21, 31). The major cellular target of RSV is the airway lining epithelial cell surface, where productive viral replication is observed in vivo and in vitro (20, 25, 28). Epithelial cells detect the presence of virus-encoded patterns via specific pathogen recognition receptors to activate arms of the innate immune response. In particular, one early signaling pathway activated by single-stranded RNA viral infection is mediated by retinoic acid-inducible gene I (RIG-I), a prototypical member of the leucine-rich RNA helicases that binds RSV RNA early in the course of infection and whose activation is required for antiviral and inflammatory signaling (28).

Upon binding single-stranded 5′-phosphorylated RNA, RIG-I undergoes a conformational change, promoting its association with E3 ubiquitin ligases, including tripartite motif-containing protein 25 and Riplet/RNF135 (34). The subsequent RIG-I ubiquitylation promotes its association with the mitochondrial activator of signaling (MAVS), resulting in MAVS oligomerization on the mitochondrial surface. Subsequent recruitment of signaling adapters, including IκB kinase γ (IKKγ) and TRAF, results in the formation of an activated signaling complex converging on the latent cytoplasmic transcription factor NF-κB, inducing its translocation into the nucleus. Although the chemistry of the MAVS ubiquitylation is not known, studies of canonical NF-κB pathway activation in response to cytokines have shown that inducible, site-specific Lys-63 ubiquitylation is a posttranslational modification required for signal adapters (IKKγ, TRAF3, and RIP1) to associate with their upstream activators (15, 26, 48).

A body of work has shown that the activity of NF-κB is tightly regulated by negative feedback systems, at the level of both expression of the IκB inhibitors and termination of the upstream signal generating kinases (reviewed in references 3 and 4). In this regard, one of the major feedback regulators important for terminating NF-κB activation, operative in response to both activated tumor necrosis factor receptor (TNFR) superfamily and RIG-I–MAVS, is a ubiquitin-modifying protein complex composed of the NF-κB-inducible A20/TNFAIP3, the E3 ubiquitin ligase Itch, and ring finger 11 proteins (27, 39, 40). The inducible formation of A20/TNFAIP3 removes Lys-63-linked ubiquitin chains and replaces them with K48-linked ubiquitin chains. This modification results in TRAF and RIP1 degradation via the proteasome pathway, thereby terminating the signal.

In response to RSV infection, NF-κB translocation is mediated by two distinct pathways, termed the canonical and cross talk pathways (4, 19, 29). The canonical pathway requires the

* Corresponding author. Mailing address: Department of Medicine, Institute for Translational Sciences, University of Texas Medical Branch (UTMB), Galveston, TX 77555-1060. Phone: (409) 772-2824. Fax: (409) 772-8709. E-mail: arbrasie@utmb.edu.

▽ Published ahead of print on 12 August 2009.

"signalsome," a multiprotein signaling complex composed of the catalytic kinases IKKα and -β, and a third adapter subunit, termed IKKγ. Upon IKK association with RIG-I–MAVS, IKKβ is phosphorylated in its activation loop, an event that induces IκBα NH_2-terminal phosphorylation, ubiquitylation, and degradation, releasing RelA to translocate into the nucleus. In recent work, we have discovered that RIG-I–MAVS directly interacts with IKKα–NF-κB-inducing kinase (NIK), producing the cross talk pathway (29). In the cross talk pathway, NIK-induced IKKα activation results in COOH-terminal cotranslational processing of the 100-kDa NF-κB2 cytoplasmic precursor, releasing associated RelA and RelB for nuclear translocation (29). Through coupling to both the canonical and cross talk pathways, RSV infection results in RelA release from several distinct cytoplasmic stores.

Studies of TNFR-induced NF-κB signaling indicate that the nuclear translocation step is necessary but not sufficient for activation of NF-κB-dependent target genes (22, 33, 44). In addition to its release, RelA is an inducible phosphoprotein at multiple regulatory sites implicated in its transcriptional activation, including Ser residues 210, 276, 529, 536, and others (2, 13, 22, 37). In response to tumor necrosis factor (TNF), a parallel, IKK-independent signaling module is also required, whose mechanism involves Ser-directed phosphorylation at amino acid 276 mediated by the catalytic subunit of protein kinase A. Ser-276 phosphorylation of RelA is required for its subsequent acetylation and functional association with p300/CBP coactivator (10, 22, 51). In addition, Ser-276 phosphorylation induces complex formation with the positive transcriptional elongation complex (P-TEFb), resulting in the activation of a subset of NF-κB-dependent genes (33). Moreover, current work has shown that signal-inducible posttranslational modifications in the NF-κB pathway are highly stimulus specific (13, 37), with phospho-Ser-276 formation being essential for TNF signaling, whereas inducible phospho-Ser-536 is required to mediate angiotensin II signaling (13). The role of phosphorylation in RSV-mediated RIG-I–MAVS signaling has not been systematically elucidated.

In this study, we examine the requirement of RelA phosphorylation in RSV-induced chemokine expression. RSV induces a time-dependent Ser phosphorylation on residues 276 and 536 in parallel with enhanced formation of reactive oxygen species (ROS). In contrast to phospho-Ser-536 formation, RSV-induced phospho-Ser-276 RelA formation is dependent on ROS signaling. Antioxidant treatments inhibit phospho-Ser-276 formation without influencing RSV replication. In the absence of Ser-276 phosphorylation, inducible RelA/NF-κB DNA-binding activity is preserved; however, RSV-induced NF-κB gene expression is significantly inhibited. RSV is a potent activator of cytoplasmic mitogen- and stress-activated protein kinase 1 (MSK1); inhibition of MSK1 by antioxidants, H89, or small interfering RNA (siRNA)-mediated knockdown inhibits RSV-induced Ser-276 phosphorylation and NF-κB-dependent gene expression. Together, these data indicate that ROS regulates MSK1, a kinase upstream of phospho-Ser-276 formation required for virus-induced NF-κB activation.

MATERIALS AND METHODS

Cell culture. Human A549 pulmonary type II epithelial cells (American Type Culture Collection) were grown in F-12K medium (Gibco, Invitrogen) with 10% fetal bovine serum, penicillin (100 U/ml), and streptomycin (100 g/ml) at 37°C in a 5% CO_2 incubator. Mouse embryonic fibroblasts (MEFs) were cultured in Eagle's minimum essential medium (Gibco, Invitrogen) with 0.1 mM nonessential amino acids, 1.0 mM sodium pyruvate, and 10% fetal bovine serum.

Virus preparation and infection. The human RSV A2 strain was propagated in Hep2 cells and purified on a sucrose cushion gradient (28, 29). Cells were infected at a multiplicity of infection (MOI) of 1.0 for the indicated times.

Quantitative real-time PCR (qRT-PCR). Total RNA was extracted using acid guanidinium-phenol extraction (TRI reagent; Sigma). One microgram of RNA was reverse transcribed using SuperScript III in a 20-μl reaction mixture. One microliter of cDNA product was diluted 1:2, and 2 μl was amplified in a 20-μl reaction mixture containing 12.5 μl of SYBR green supermix (Bio-Rad) and 0.2 μM each of forward and reverse gene-specific primers; aliquoted into 96-well, 0.2-mm thin-wall PCR plates; and covered with optical-quality sealing tape. The plates were denatured for 90 s at 95°C and then subjected to 40 cycles of 15 s at 94°C, 60 s at 60°C, and 1 min at 72°C in an iCycler (Bio-Rad). After PCR was performed, PCR products were run on 2% agarose gels to assure a single amplification product. Statistical analysis of gene expression was performed using the threshold cycle method, as described earlier (28, 29). Primers are described in reference 33.

Assessment of cellular redox state. Changes in intracellular ROS were determined by measurement of oxidation of 2,7-dichlorodihydro-fluorescein diacetate (H_2DCF-DA; Molecular Probes), as we described previously (22). Briefly, cells at 70% confluence were infected with RSV (MOI, 1.0 per cell) or mock infected. At the indicated times, both mock- and RSV-infected cells were loaded with 50 μM (final concentration) H_2DCF-DA for 15 min at 37°C. Changes in dichlorofluorescein (DCF) fluorescence intensities were determined with an FLx800 microplate fluorescence reader (BioTek Instruments, Inc., Winooski, VT) at excitation (485-nm) and emission (528-nm) wavelengths. In selected studies, fluorescence intensities (excitation, 505 nm; emission, 535 nm) were confirmed by flow cytometry (Becton Dickinson FACScan; San Jose, CA). Each data point represents the mean fluorescence results for 12,000 cells from three or more independent experiments, with data expressed as means ± standard errors of the means (SEM).

To assess glutathione (GSH)/oxidized GSH (GSSG) ratios, parallel cultures were infected with RSV (or were mock infected) at an MOI of 1. GSH/GSSG ratios were determined at 0, 6, 15, and 24 h after infection using the Bioxytech GSH/GSSG-412 (OxisResearch, Portland, OR) assay kit, according to the manufacturer's protocol. From mock- and RSV-treated cells, the reduced GSH samples were obtained with a cold metaphosphoric acid extraction, while the GSSG was prepared using the same type of extraction after scavenging free thiols with 1-methyl-2-vinylpyridinium trifluoromethanesulfonate. GSH reductase, NADPH, and chromogen were added to each sample, and the absorbance at 412 nm was monitored for 3 min. GSH standards were prepared from a 1 mM stock solution in 10% (wt/vol) metaphosphoric acid.

Western immunoblotting. Whole-cell extracts (WCEs) were prepared using modified radioimmunoprecipitation assay buffer (50 mM Tris-HCl [pH 7.4], 150 mM NaCl, 1 mM EDTA, 0.25% sodium deoxycholate, 1% Igepal CA-630, 1 mM phenylmethylsulfonyl fluoride, 1 mM NaF, 1 mM Na_3VO_4, and 1 μg/ml each of aprotinin, leupeptin, and pepstatin). Proteins were fractionated by 8% sodium dodecyl sulfate-polyacrylamide gel electrophoresis (SDS-PAGE) and transferred to a polyvinylidene difluoride membrane by electroblotting. Membranes were blocked in 5% nonfat dry milk in Tris-buffered saline-0.1% Tween and probed with the indicated primary antibody (Ab). Membranes were washed and incubated with IRDye 700-conjugated anti-mouse Ab or IRDye 800-conjugated anti-rabbit Ab (Rockland, Inc.). Finally, the membranes were washed three times with Tris-buffered saline-0.1% Tween and imaged by an Odyssey infrared scanner. The sources of primary Abs were anti-Flag M2 monoclonal Ab (Stratagene), anti-RelA polyclonal Ab (Santa Cruz), and anti-phospho-MSK1 Ab (Cell Signaling).

siRNA-mediated gene silencing. Scrambled or human MSK1 siRNAs were commercially obtained (Dharmacon Research, Inc., Lafayette, CO) and transfected into A549 cells using TransIT-siQuest transfection reagent (Mirus Bio Corp., Madison, WI), according to the manufacturer's instructions.

MSK1 assay. MSK1 activity was measured by immunoprecipitation (IP)-kinase assays with WCEs, as described previously (32). Briefly, A549 WCEs were prepared by lysis in a buffer containing 50 mM Tris-HCl (pH 7.5), 1 mM EGTA, 1 mM EDTA, 1% Triton X-100, 0.27 M sucrose, 0.1% (vol/vol) β-mercaptoethanol, 1 mM sodium orthovanadate, 50 mM sodium fluoride, 5 mM sodium pyrophosphate, complete proteinase inhibitor cocktail (Sigma-Aldrich), and 1 mM phenylmethylsulfonyl fluoride. The lysate was sonicated and centrifuged at 14,000 × *g* for 10 min at 4°C. For MSK1 IP, 0.5 mg of cell lysate was precleared with protein A-agarose beads (Sigma-Aldrich) and immunoprecipitated with 5

μg of rabbit anti-MSK1 Ab (Santa Cruz Biotech) and 20 μl of protein A-agarose beads (50% slurry) for 4 h at 4°C. The immune complex was washed twice with high-salt washing buffer (50 mM Tris-HCl [pH 7.5], 0.5 M sodium chloride, 0.1 mM EGTA, and 0.1% β-mercaptoethanol) and once with kinase reaction buffer (50 mM Tris-HCl [pH 7.5], 0.1 mM EGTA, 0.1% β-mercaptoethanol). The kinase reaction was conducted in 50 mM Tris-HCl (pH 7.5), 0.1 mM EGTA, 0.1% β-mercaptoethanol, 2.5 μM protein kinase inhibitor, 30 μM Crosstide peptide (GRPRTSSFAEG), 10 mM MgAc, and 0.1 mM [γ-^{32}P]ATP in a total volume of 30 μl for 20 min at 30°C. The reaction was stopped by transferring content to P81 filter paper, washed with 75 mM orthophosphoric acid, and radioactivity counted. After background subtraction, MSK1 activity was determined by dividing the radioactivity from the RSV-infected sample by that of the 0-h sample (mock infection) and expressed as level of induction over uninfected cells.

RESULTS

RSV induces RelA Ser-276 and Ser-536 phosphorylation. Previously we have shown that RSV infection results in activation of RelA/NF-κB in lung epithelial cells by promoting its translocation from the cytoplasmic compartment to the nucleus via proteolysis of its inhibitor IκBα, by pathways distinct from those induced by the prototypical TNF activator (23). Because RelA Ser phosphorylation is required for activating its transactivation potential for inducing target gene expression (2, 22, 33, 51, 52) and is under stimulus-specific control, we have investigated its role in RelA activation in response to RSV infection.

For this goal, we initially observed the kinetics of RelA phosphorylation in response to RSV infection in human A549 epithelial cells. We focused on epithelial cells because RSV primarily replicates in alveoli and bronchiolar epithelium in fatal human cases of RSV bronchiolitis and are therefore a relevant model of human infection (46). A549 cells were selected because these cells express surfactant and tannic acid-positive lamellar bodies characteristic of type II alveoli and are permissive for RSV replication (17, 23, 24). In order to observe the kinetics of RelA phosphorylation in response to RSV infection, A549 cells were infected with RSV (MOI, 1.0) for 0 to 24 h. RelA phosphorylation was determined in WCEs by Western immunoblot assays using phospho-Ser-selective Ab. We observed that phospho-Ser-276 RelA was faintly detectable in uninfected cells but, upon RSV infection, showed a time-dependent increase in immunostaining, first detectably increasing at 6 h and continuing to increase over 24 h (Fig. 1A). Phospho-Ser-536 RelA formation increased in a similar pattern (Fig. 1A, middle). Because these increases were independent of changes in total RelA abundance, these data indicated to us that RSV induces RelA phosphorylation at multiple sites.

To determine the intracellular localization of phospho-Ser-276 RelA, we repeated the RSV assay over time, fractionating the cells into cytoplasmic and nuclear fractions using an established sucrose gradient purification technique (16). The phospho-Ser-276 RelA could be detected in both the cytoplasmic and nuclear fractions.

RSV induces intracellular ROS formation. ROS are recognized to be potent intracellular signaling messengers in response to cytokine stimulation and viral infection (7, 22). To establish the kinetics of RSV-induced ROS formation, the kinetics of intracellular oxidation of DCF-DA was measured in RSV-infected A549 cells (MOI, 1). We observed that RSV induced a rapid, transient peak of DCF fluorescence, peaking within 2 h of viral adsorption (Fig. 2A). This oxidative stress then fell to ~3-fold above that of mock-infected cells until 6 h after infection, whereupon a steady increase in DCF formation was observed, showing an apparent plateau of 7-fold-higher induction until the termination of the experiment (24 h) (Fig. 2A). As an independent measure of cellular oxidation, the ratio of reduced-to-oxidized glutathione (GSH/GSSG) was measured under the same experimental condition. Under basal conditions, the GSH/GSSG ratio was ~27, which fell to 13 after 2 h of RSV exposure. Although the GSH/GSSG ratios increased 3 to 4 h after viral adsorption, it steadily fell at 6 h and later times. Examination of the GSH/GSSG ratio over time indicated a close inverse relationship between the GSH/GSSG ratio and DCF formation (cf. Fig. 2A and B).

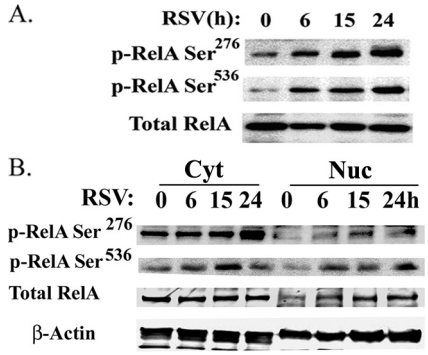

FIG. 1. RSV induces RelA phosphorylation in A549 cells. (A) Human type II alveolar carcinoma A549 cells were infected with RSV (MOI, 1.0) for 0, 6, 15, and 24 h, and WCEs were prepared. Equal amounts of lysate (100 μg protein) were separated on an 8% SDS-PAGE gel, transferred to a polyvinylidene difluoride membrane, and probed with anti-phospho-Ser-276 RelA (p-RelA Ser^{276}) or phospho-Ser-536 RelA (p-RelA Ser^{536}) Abs. The membrane was incubated with anti-RelA Ab (Total RelA) to show equal loading. (B) RSV-infected A549 cells were fractionated into cytoplasmic (Cyt) and nuclear (Nuc) preparations for analysis by Western blotting using the indicated Abs. Each experiment was repeated twice, and data from a representative experiment were shown.

To experimentally modulate the ROS stress, we tested the effect of two chemically unrelated agents on RSV-infected A549 cells. For this experiment, we selected dimethyl sulfoxide (DMSO), a free radical scavenger, and *N*-acetyl cysteine (NAC), an antioxidant. Addition of DMSO (2%, vol/vol) to the culture medium significantly reduced the formation of GSSG (Fig. 2C). We have previously shown that DMSO at these concentrations (from 0 to 4%) produces no detectable effects on cell toxicity measured by cell numbers or apoptosis, determined by annexin V staining, nor is there measureable effect on inducible JNK or p38 MAPK activity (22). Similarly, treatment with NAC (15 mM) also significantly inhibited RSV-induced ROS generation throughout the course of the experiment (6 to 24 h) (Fig. 2D). Together, these findings indicate that RSV induces enhanced ROS stress that can be experimentally reversed.

ROS mediates RelA Ser-276 phosphorylation. Because the time scales for ROS formation and RelA phosphorylation were similar, we sought to test whether virus-inducible intracellular ROS is linked to inducible RelA phosphorylation. For this purpose, A549 cells were infected with RSV in the absence or

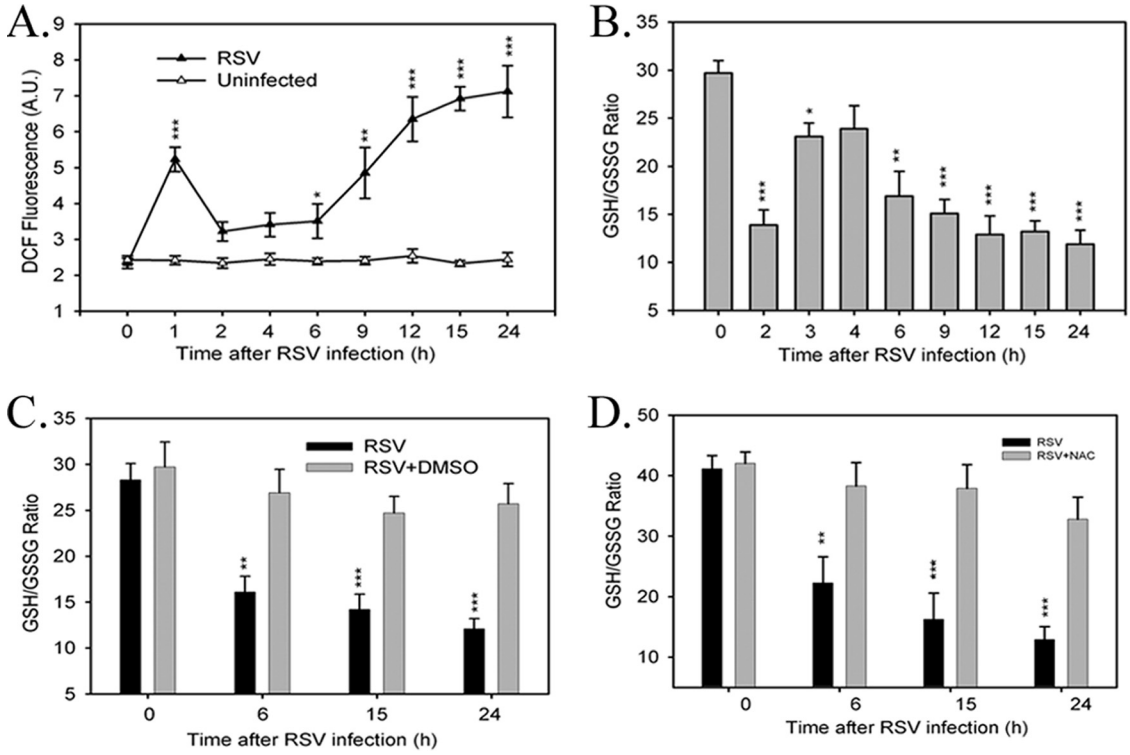

FIG. 2. RSV induces ROS stress in a time-dependent manner. (A) RSV-induced changes in cellular ROS levels. At the times indicated, RSV-infected cells were loaded with H_2DCF-DA, and changes in DCF fluorescence were assessed by flow cytometry. A.U., arbitrary units. (B) Kinetic changes in GSH oxidation in RSV-infected cells. GSH/GSSG ratios were determined, as described in Materials and Methods. (C, D) RSV-infected cells were treated with DMSO (2%) or NAC (15 mM), and GSH/GSSG ratios were determined. All results are the means ± SEM ($n = 4$ to 7). *, $P > 0.05$; **, $P = 0.01$; ***, $P > 0.001$.

presence of effective concentrations of antioxidants, NAC (15 mM), or DMSO (2%, vol/vol). Cells were harvested 15 h after infection, and the formation of phospho-Ser-276 RelA was determined by Western immunoblotting. Strikingly, NAC significantly reduced the RSV increase in phospho-Ser-276 RelA formation (Fig. 3A, top). Similarly, DMSO had a similar effect on inhibiting the formation of phospho-Ser-276 (Fig. 3A, bottom). In contrast, phospho-Ser-536 RelA formation was not consistently affected (Fig. 3B). To exclude the possibility that NAC or DMSO affected viral replication, we measured RSV transcription in the presence or absence of NAC or DMSO. For this purpose, we measured the transcription of RSV N, a gene absolutely required for RSV replication (12). We observed that cellular treatment with either NAC or DMSO had no effect on RSV N mRNA expression (Fig. 3C). Next, we examined the effect of NAC and DMSO on RSV-inducible NF-κB binding by electrophoretic mobility shift assay (EMSA). In uninfected cells, a weak NF-κB1/p50 band is seen; however, in response to RSV infection, an increase in the NF-κB1/p50 and the RelA-p50 heterodimer complexes is clearly seen (Fig. 3D) (note that we have shown this upper complex is sequence specific and composed of RelA by supershifting and oligonucleotide affinity pull-down experiments [22, 23, 42]). Figure 3D shows that there was inducible p50/p50 and p50/RelA binding to κB sites in response to RSV infection. However, NAC and DMSO treatment failed to inhibit RSV-induced NF-κB binding (Fig. 3D). In addition, the RSV-induced nuclear translocation of RelA was unaffected by NAC and DMSO in RSV-infected cells by Western blotting (data not shown).

A subset of RSV-inducible NF-κB-dependent gene expression is antioxidant sensitive. Since the RSV replication and RSV-induced DNA binding of RelA is intact in antioxidant-treated cells, this allowed us to test the role of phospho-Ser-276 RelA in mediating virus-inducible chemokine expression. A549 cells pretreated in the absence or presence of NAC (15 mM) or DMSO (2%) were RSV infected (MOI, 1) for different amounts of time. The expression of NF-κB-dependent interleukin-8 (IL-8), Gro-β, and IκBα genes was measured by qRT-PCR. These genes were selected to represent a subset of the phospho-Ser-276 RelA-dependent (IL-8, Gro-β) and -independent genes downstream of TNF signaling (33). We observed that RSV infection alone increased IL-8 expression by ~50-fold at 6 h and ~580-fold at 24 h (Fig. 4A). In the presence of NAC or DMSO, IL-8 expression was reduced to less than half throughout the 24-h experiment (P was <0.01 compared to RSV-infected cells alone) (Fig. 4A). Similar results were found with RSV-inducible Gro-β expression where Gro-β was induced by ~5-fold at 6 h and ~50-fold at 24 h after viral adsorption over mock-infected cells (Fig. 4B). In the presence of either NAC or DMSO, RSV-inducible Gro-β expression was significantly reduced throughout the 24-h time course experiment (Fig. 4B). In contrast, RSV-inducible IκBα gene expression was unaffected by antioxidant treatment (Fig. 4C). Together, these data suggested that virus-induced ROS

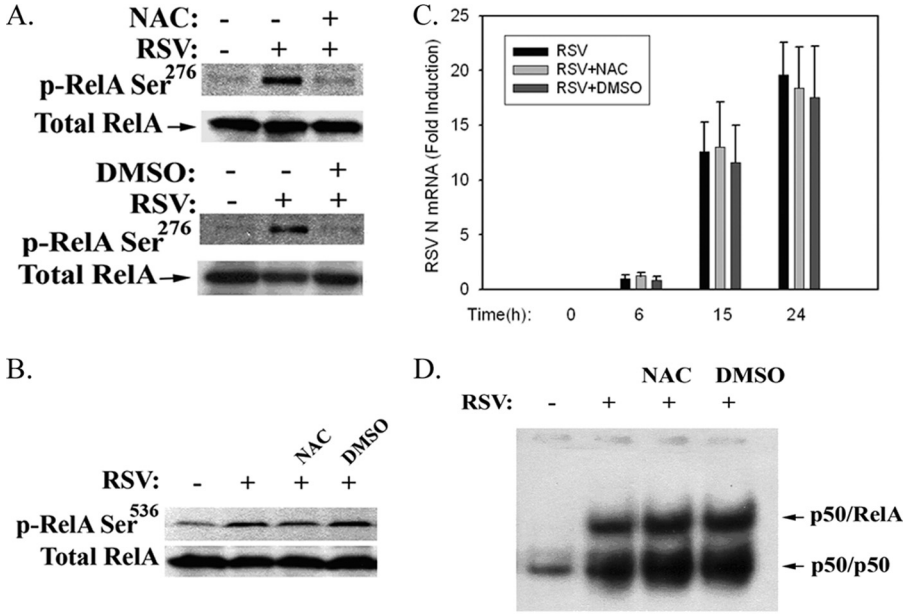

FIG. 3. RSV-inducible phospho-Ser-276 RelA formation is antioxidant sensitive. (A) A549 cells preincubated with NAC (15 mM; top) or DMSO (2%; bottom) for 1 h were RSV infected for 15 h (MOI, 1). A Western immunoblot of RelA Ser-276 phosphorylation is shown. Total RelA was assayed as a loading control. p-RelA Ser^{276}, phospho-Ser-276 RelA; p-RelA Ser^{536}, phospho-Ser-536 RelA. (B) Cells treated as described in Fig. 3A were fractionated by SDS-PAGE, and formation of RelA Ser-536 phosphorylation was measured by Western immunoblotting. (C) NAC (15 mM)- or DMSO (2%, vol/vol)-pretreated A549 cells were RSV infected, and total cellular RNA was extracted. Results from the qRT-PCR assay for expression of RSV N transcripts are shown. The bars represent means ± SEM of results from triplicate samples. (D) A549 cells were treated as described in Fig. 3A, and nuclear extracts were prepared. An autoradiogram from an EMSA using the radiolabeled NF-κB duplex is shown. The identities of the NF-κB complexes are indicated (p50/p50 and p50/RelA).

controlled a pathway required for RelA Ser-276 phosphorylation and activation of a subset of NF-κB-dependent genes, a subset that included inflammatory chemokine genes.

RSV induces cytoplasmic MSK1 activity in an ROS-dependent manner. Recent studies have indicated that MSK1 mediates NF-κB activation in response to cytokine stimulation. We therefore examined if RSV infection activated MSK1 in A549 cells using two separate approaches. First, we measured the phosphorylation of MSK1 at Ser residue 376, a critical phosphorylation in its activation (32). WCEs prepared from RSV-infected A549 cells at the indicated times were assayed by Western immunoblotting, probing anti-phospho-Ser-376 MSK1 Ab. A parallel TNF alpha (TNF-α) stimulation was performed as a positive control. In the absence of RSV infection, phospho-Ser-376 MSK1 was undetectable, increasing at 6 h of RSV infection and plateauing from 15 to 24 h of infection (Fig. 5A, top, left). Reprobing the membrane for total MSK1 indicated that RSV had no effect on total MSK1 protein abundance (Fig. 5A, middle). Here, we also noted the induction of phospho-Ser-276 RelA closely paralleled MSK1 activation kinetics, as well as that of ROS induction (compare Fig. 2A and 5A). To determine whether RSV induced a different level of phospho-Ser-376 MSK than that of TNF-α, the ratio of phospho-MSK1 was quantified by infrared scanning, and the percentage of phospho-MSK1 was calculated (Fig. 5A, bottom). Here, the amount of phospho-MSK formation between the two treatments was similar, although the kinetics of MSK1 activation between the two stimuli differed.

Second, we measured directly MSK1 by IP-kinase assay, measuring incorporation of [γ-^{32}P]ATP into a synthetic peptide substrate (CREBtide; see Materials and Methods). IP-kinase assays were performed in mock-infected and RSV-infected cells treated in the absence or presence of antioxidants, where MSK1 activity was expressed as percentage of radiolabel incorporation over mock-infected cells. RSV infection enhanced phospho-CREBtide incorporation to ~300% compared to that of mock-infected IPs (Fig. 5B). The exposure of either NAC or DMSO strongly inhibited MSK1 activity to nearly those of control values.

Early work with fibroblasts has shown that MSK1 is a nuclear-localized kinase responsive to cytokine stimulation (43); however, its location in epithelial cells and the effects of virus infection on subcellular distribution are not known. To further understand its regulation, A549 cells were fractionated into cytoplasmic and sucrose cushion-purified nuclear extracts using our established protocols (16). Matched cellular equivalents of cytoplasmic and nuclear proteins were assayed by Western blotting using anti-pan-MSK1 and anti-phospho-Ser-376 MSK1 Abs. Surprisingly, the majority of total MSK1 was cytoplasmic in localization (Fig. 5C, bottom) Similarly, phospho-Ser-376 MSK1 was primarily cytoplasmic, and a weak nuclear translocation of phospho-Ser-376 MSK1 was observed at 6 and 15 h after RSV infection (Fig. 5C, top). To confirm that the nuclear extracts were intact and that the cytoplasmic MSK1 staining was not due to nuclear leakage, we stained them with the nuclear protein lamin B, whose staining was exclusively localized in the nuclear fraction. Together, these data indicate that RSV induces activation of cytoplasmic MSK1 activity in an ROS-dependent manner.

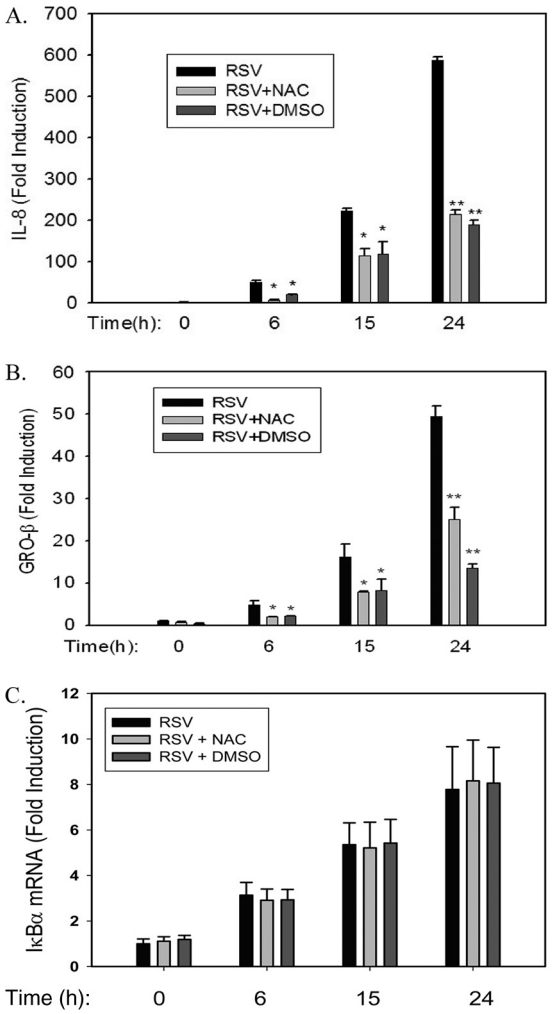

FIG. 4. RSV-induced NF-κB-mediated chemokine gene expression is antioxidant sensitive. (A) A549 cells treated as described in Fig. 3 were RSV infected at the indicated times prior to total RNA extraction. Measurement of IL-8 mRNA expression by qRT-PCR is shown. Each bar represents the mean ± SEM of results from triplicate samples from an experiment repeated twice. *, $P < 0.01$; **, $P < 0.001$. (B) Gro-β expression was measured in the same samples. (C) IκBα expression was measured in the same samples.

Stimulus specificity of ROS inducers on MSK1 activation and phospho-Ser-276 RelA formation. Previously, we demonstrated that TNF stimulation induces a spike in intracellular ROS (22). To establish whether MSK1 activation was produced in response to other ROS-inducing agents, we compared the responses to TNF and H_2O_2. Relative to the effects of RSV, TNF administration produces a rapid rise in DCF oxidation, peaking at 1 h after stimulation and returning to baseline (Fig. 6A). A second peak of ROS production was observed, consistent with the oscillatory behavior of the TNF-induced NF-κB signal (reviewed in reference 4). In contrast, administration of extracellular H_2O_2 also produced a sharp monotonic peak in ROS (Fig. 6B). To determine the effects of these ROS-inducing agents on MSK1 activity and phospho-Ser-276 RelA formation, WCEs were prepared from replicate experiments and subjected to Western immunoblotting. Although TNF induced a rapid formation of phospho-Ser-276 RelA and parallel MSK1 activation, H_2O_2 did not (Fig. 6C). Together, these data indicate that the MSK1–phospho-Ser-276 RelA pathway is activated by intracellular ROS generation.

MSK1 inhibition blocks phospho-Ser-276 RelA formation and NF-κB-dependent gene expression. Our findings that MSK1 activity and RelA Ser-276 phosphorylation were both inhibited by antioxidants led us to suspect that MSK1 may be the RelA Ser-276 kinase responsible for RelA activation in response to RSV infection. To further test this hypothesis, we investigated the effect of a known MSK1 inhibitor, H-89 (43). First, we examined the MSK1 activation and RelA Ser-276 phosphorylation in RSV-infected cells in the presence of increasing doses of H-89 (from 10 to 20 μM). We observed that the RSV-induced phospho-Ser-376 MSK1 formation was inhibited by H-89 in a dose-dependent manner (Fig. 7A, top). In parallel, formation of phospho-Ser-276 RelA was inhibited (Fig. 7A, bottom). Similarly, H-89 significantly reduced the RSV-induced activation of the IL-8 and Gro-β genes (Fig. 7B and C). These results are consistent with MSK1 playing a key role in RSV-induced phopho-Ser-276 RelA formation and target gene expression.

siRNA-mediated MSK1 knockdown inhibits RSV-induced chemokine expression. To more definitively investigate the role of MSK1 in RSV-induced signaling, we performed siRNA-mediated MSK1 knockdown. A549 cells were transfected for 48 h with scrambled siRNA or MSK1-targeted siRNA and were then RSV infected (MOI of 1, 15 h). The silencing effect of siRNAs was determined in WCEs by Western immunoblotting. We observed that transfection with scrambled siRNA had no effect on the RSV-induced phospho-Ser-376 MSK1 formation, whereas transfection with anti-MSK1 siRNA produced a ~75 to 80% decrease in both phospho-Ser-376 MSK1 and total MSK1 levels (Fig. 8A). In parallel, the formation of phospho-Ser-276 RelA was also reduced (Fig. 8A, middle).

Next, we determined the effect of MSK1 silencing on RSV-induced Gro-β and IL-8 expression by qRT-PCR. In this experiment, RSV infection caused a ~200-fold induction of IL-8, whereas a ~60-fold induction was observed in response to MSK1 knockdown (note that the level of induction varies from experiment to experiment because the expression of these cytokines is close to the assay detection limit) (Fig. 8B). Similarly, RSV induced a ~1,300-fold induction of Gro-β that was significantly reduced after MSK1 knockdown (Fig. 8C). These data further support the role of MSK1 in RSV-induced RelA activation and chemokine expression.

RelA Ser-276 phosphorylation is required for RSV-inducible gene expression. Finally, to directly demonstrate the requirement of Ser-276 phosphorylation on RSV-induced RelA activation, we examined the effect of RSV on a RelA Ser-to-Ala site mutation of residue 276 (S276A). For this purpose, we investigated a RelA-deficient background using $RelA^{-/-}$ MEFs. $RelA^{-/-}$ MEFs stably transfected with either the RelA wild type (WT) or the RelA S276A mutation were infected with RSV from 0 to 24 h, and Gro-β expression was measured by qRT-PCR. We found that RSV infection induced Gro-β expression in a time-dependent manner in RelA WT-expressing cells, whereas Gro-β expression was dramatically reduced in cells expressing the RelA S276A mutation (Fig. 9).

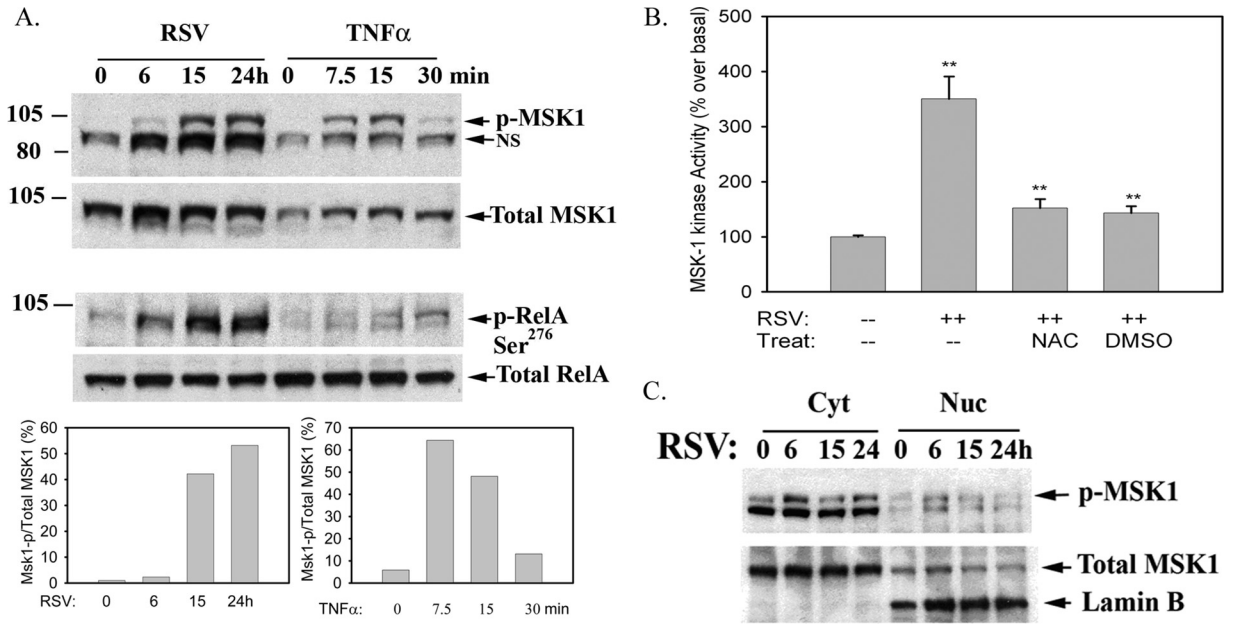

FIG. 5. RSV infection induces MSK1 activity. (A) A549 cells were infected with RSV for 0, 6, 15, and 24 h. Top, 100 μg of WCE was fractionated by SDS-PAGE, and phospho-Ser-376 MSK1 (p-MSK1) formation was determined by Western immunoblotting using a phospho-specific Ab (top, left). TNF-α stimulation (20 ng/ml) was assayed at the indicated times as a positive control (top, right). NS, nonspecific band. The locations of molecular mass markers are shown on the left. Total MSK1 was measured as a loading control. Middle, WCEs from the same experiment were assayed for phospho-Ser-276 (p-RelA Ser^{276}) and total RelA using cognate Abs. Bottom, the ratio of phospho-MSK was determined as a percentage of total MSK1 staining for each blot. (B) RSV-induced MSK1 kinase activity. IP-kinase activity of WCEs from control cells, RSV-infected cells, or RSV-infected cells in the presence of NAC (15 mM) or DMSO (2%). Incorporation of [γ-^{32}P]ATP into CREBtide is reported as a percentage of that from uninfected WCEs. Each bar is the mean ± SEM of results from three replicates. The experiment was repeated twice. **, $P < 0.001$. (C) MSK1 subcellular distribution. Cytoplasmic (Cyt) and sucrose cushion-purified nuclear (Nuc) extracts were prepared from RSV-infected A549 cells at the indicated times (MOI, 1). Equal cellular equivalents of protein were fractionated by SDS-PAGE. A Western immunoblot for phospho-Ser-376 MSK1 and total MSK1 abundance is shown. Bottom, the same membrane was probed with lamin B Ab as a marker for nuclear extract integrity.

DISCUSSION

RSV is a major cause of epidemic lower respiratory disease in children worldwide that disproportionately affects those with underlying bronchopulmonary dysplasia or with impairments in innate immunity, including immunodeficiency or cystic fibrosis (5). Although the pathogenesis of severe disease is not fully understood, it is known that RSV primarily replicates in lower airway bronchiolar and alveolar epithelial cells (46). Here, RSV replication results in the activation of mucosal innate immunity and inflammation by inducing NF-κB signaling to activate networks of inflammatory cytokines (19, 23, 42, 49). Previous work by our group has shown that early in the process of RSV replication, a major intracellular sensor of RSV infection is the cytoplasmic RIG-I helicase, whose ubiquitylation and association with MAVS generates multiple signals converging on the NF-κB pathway (28). Most of this work has focused on NF-κB translocation, an event trigged by its release from cytoplasmic p100 and IκBα inhibitors (23, 29), which is necessary, but not sufficient, for NF-κB activation. Here we provide, for the first time, evidence for a virus-induced ROS-initiated pathway, activating the cytoplasmic MSK1 converging on phospho-Ser-276 RelA formation and target gene expression.

NF-κB is inducibly phosphorylated on multiple sites in a stimulus- and cell type-specific manner, a posttranslational modification that, depending on the site, affects protein interaction, transactivation potential, subcellular distribution, DNA-binding site recognition, and acetylation (2, 10, 13, 22, 33, 37, 45, 52). Here, we observe that although RSV induces phospho-Ser-536 and phospho-Ser-276 RelA formation with similar kinetics, Ser-276 phosphorylation was uniquely sensitive to treatment with antioxidants. Our studies and others have shown that RSV induces cellular ROS stress measured by DCF-DA oxidation and the reversal of GSH/GSSG ratios (8, 30). ROS stress appears to be a common cellular response to RNA virus infections, where it may play a role as a secondary messenger (38). Viral infection-induced ROS was first demonstrated in influenza infection, where ROS production increases phagocytic activity in monocytes/macrophages (36). Because functional oxidase expression in nonphagocytic cells was not initially appreciated, inducible ROS formation in epithelial cells has only more recently been investigated where its formation plays a role in mediating intracellular signaling. In this regard, we earlier reported that RSV infection induces ROS production by lung epithelial cells in vitro and in vivo through activation of an NADPH-like oxidase (7).

RSV-induced ROS affects several major signaling targets. In the RSV-infected epithelial cells, ROS formation inhibits protein phosphatase activity, resulting in activation of STAT and IRF transcription factors (7, 30). However, the role of virus-inducible ROS in the NF-κB signaling pathway has not been fully explored. Here, in a detailed study of ROS production

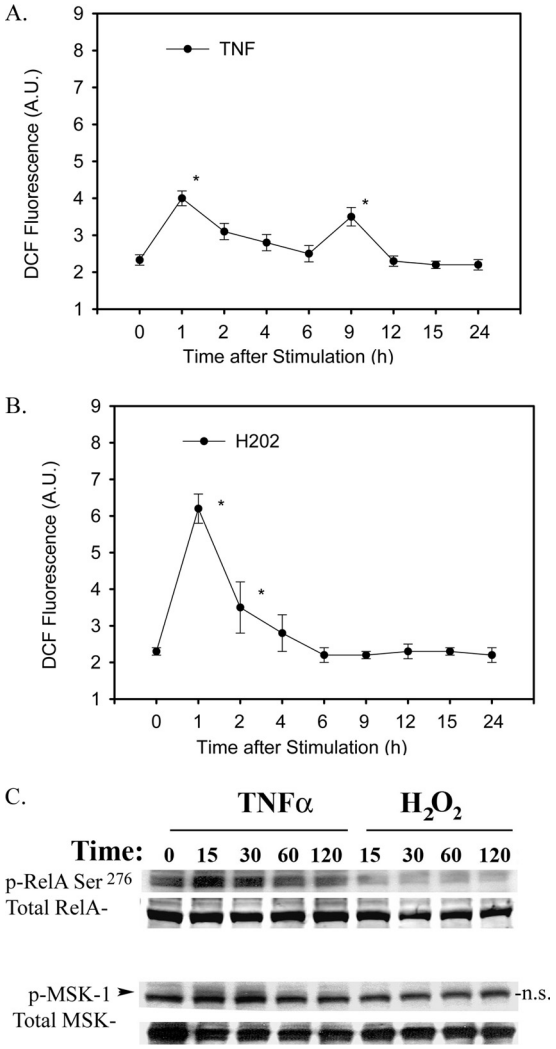

FIG. 6. Specificity of MSK1 induction by ROS. (A) A549 cells were stimulated with TNF-α (20 ng/ml) at the indicated times and loaded with H_2DCF-DA, and changes in DCF fluorescence were measured. Relative changes in DCF oxidation by flow cytometry are shown. *, $P < 0.01$; A.U., arbitrary units. (B) ROS induction by 100 μM H_2O_2. DCF oxidation was measured as described in panel A. (C) Induction of MSK1 by TNF-α and H_2O_2. WCEs were fractionated by SDS-PAGE. Abundance of total MSK1, phospho-Ser-376 MSK1 (p-MSK1), and phospho-Ser-276 RelA (p-RelA Ser^{276}) was measured by Western blotting. n.s., nonspecific band.

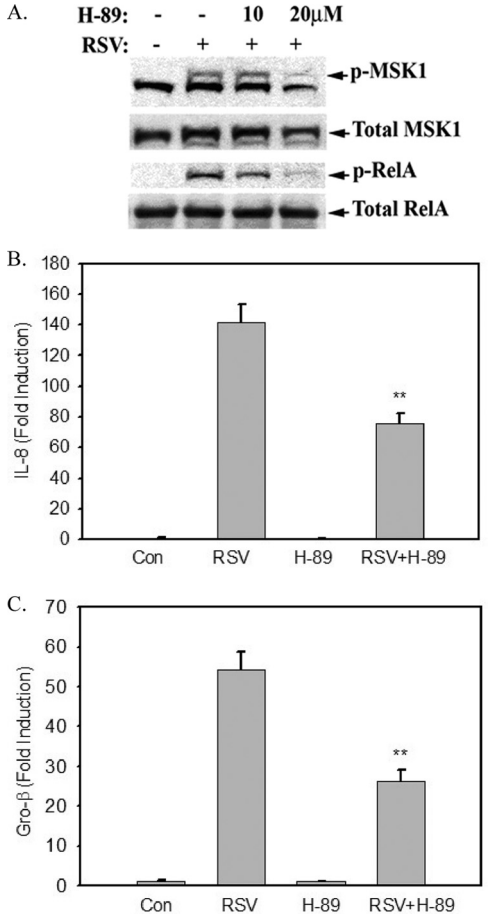

FIG. 7. MSK1 inhibitor H89 inhibits RSV-induced MSK1 phosphorylation and RelA Ser-276 phosphorylation. (A) Cells were preincubated with H89 at the indicated concentrations for 1 h and RSV infected (MOI, 1; 15 h). MSK1 phosphorylation (p-MSK1) and RelA phosphorylation (p-RelA) were determined by Western blotting with specific Abs. The same blots were probed to detect total MSK1 or RelA, respectively. (B) Effect of H89 on RSV-inducible IL-8 expression. A549 cells treated as described in Fig. 6A were extracted for total cellular RNA. The results of qRT-PCR for IL-8 mRNA are shown. *, $P < 0.05$; **, $P < 0.01$ (compared to RSV-infected cells); Con, control. (C) Effect of H89 on RSV-inducible Gro-β. The experiment was performed as described in Fig. 6B, but with qRT-PCR testing for Gro-β.

over time, we note that RSV induces a biphasic oxidative stress in epithelial cells, producing an early peak (2 to 3 h) of ROS production, a time coincident with viral attachment and internalization, and a second, sustained peak of ROS production coincident with the first round of viral replication (6 to 12 h). Our data indicates that the second, more sustained peak of ROS formation acts as a secondary messenger in the NF-κB activation pathway, converging on RelA phosphorylation at Ser-276. That the ROS-phospho-Ser-276 RelA pathway is a pathway that functions independent of NF-κB cytoplasmic release is indicated by efficient NF-κB binding in EMSAs in antioxidant-treated cells. To us, this finding suggests that a parallel NF-κB activation module exists, independent of the pathway controlling IκBα and p100 degradation and of that controlling RelA Ser-536 phosphorylation.

In this study, we have observed that RSV infection increases MSK1 activity in an intracellular ROS-dependent manner. MSK1 is expressed abundantly in all tissues and is a Ser/Thr-directed protein kinase downstream of the extracellular signal-regulated kinases 1 and 2 (ERK1/2) and p38 MAPKs that play key roles in the immune response, cell proliferation, and apoptosis (14). The MSK1 COOH terminus is an autoregulatory domain, whose phosphorylation on multiple sites allows NH_2 kinase activity toward its substrate CREB and ATF1 transcription factors (47). Our work indicates that RSV induces MSK1 activation coincident with phosphorylation of Ser-376; however, the role of other phosphorylation sites will need to be further investigated. The effect of H89 and siRNA-mediated knockdown of MSK1 both indicate that MSK1 is required for

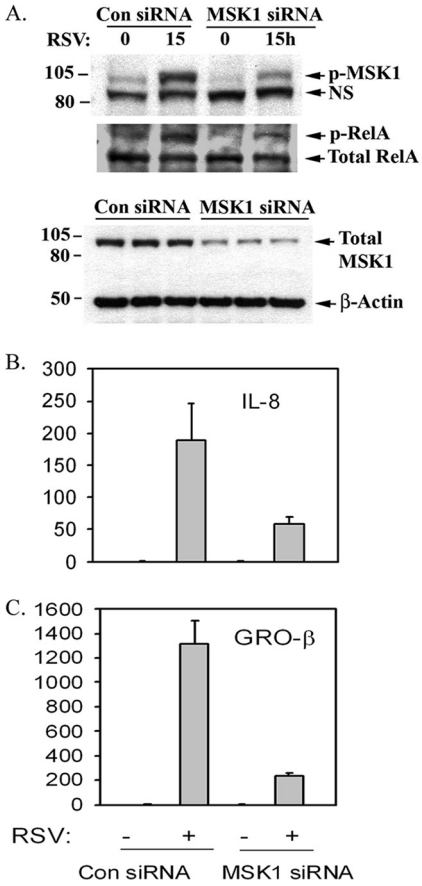

FIG. 8. Effect of siRNA-mediated MSK1 knockdown. (A) A549 cells were transfected with 100 nM scrambled siRNA (Con siRNA) or siRNA directed against MSK1 (MSK1 siRNA) for 48 h, followed by RSV infection (MOI, 1; 15 h). Top two panels, 100 μg WCE was assayed for phospho-Ser-376 MSK1 (p-MSK1) abundance by Western blotting. A separate blot loaded with extract from the same experiment was probed with anti-phospho-Ser-276 RelA or pan-RelA (p-RelA) Ab. Bottom panel, effect of MSK1 knockdown was determined by Western blotting. Three plates of A549 cells were transfected with 100 nM scrambled or MSK1 siRNA. One hundred micrograms of WCE was assayed for total MSK1 and β-actin staining by Western blotting. (B) A549 cells treated as described in Fig. 7A were extracted for total cellular RNA. IL-8 expression was measured by RT-PCR. Each bar represents the mean ± SEM of results from triplicate samples. (C) Gro-β expression was measured in the samples, as described in Fig. 7B. Each experiment was repeated twice.

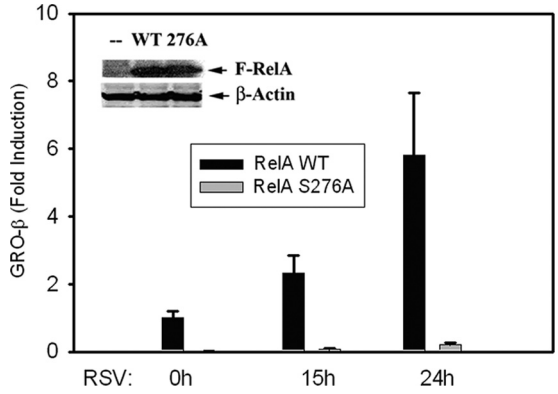

FIG. 9. Requirement of RelA Ser-276 in RSV-inducible cytokine expression. RelA$^{-/-}$ MEFs stably transfected with eukaryotic expression vectors encoding the RelA WT or RelA Ser-276–to–Ala mutation were RSV infected at the indicated times. Gro-β expression in total cellular RNA was measured by qRT-PCR. Inset, Western immunoblot of RelA WT and RelA Ser-276–to–Ala expression. −, no transfection; WT, WT RelA; 276A, the Ser-276–to–Ala RelA mutant.

inducible RelA Ser276 phosphorylation and activation of target genes. Our observations that ROS inhibition by antioxidants attenuate MSK1 activity induced by RSV is consistent with the findings of others that oxidative stress increases MSK1 activity (1). The molecular basis of ROS-dependent activation of MSK1 in RSV-infected cells is unknown. Further study will be necessary to dissect the mechanism of ROS-dependent MSK1 activation.

We have previously shown that RSV infection results in expression of 17 distinct C, CC, and CXC chemokines in lung epithelial cells (49). Pathway perturbation studies have shown that expression of the neutrophilic chemotactic factors IL-8 and Gro-β is primarily NF-κB translocation dependent (41, 42). In this study, we have discovered that induction of NF-κB translocation is not sufficient for their expression but, rather, that RSV-induced ROS-mediated RelA phosphorylation at Ser-276 by MSK1 is also required for their induction. This conclusion is supported by several sets of experimental evidence, as follows. (i) Chemically unrelated antioxidants inhibit MSK1 enzymatic activity, inducible RelA Ser-276 phosphorylation, and IL-8 and Gro-β expression. (ii) siRNA-mediated downregulation of MSK1 inhibits Ser-276 phosphorylation and also reduces expression of IL-8 and Gro-β. (iii) RelA-deficient MEFs expressing the RelA S276A mutant are unable to induce Gro-β in response to RSV infection (Fig. 9). These results strongly suggest that RSV-induced RelA Ser-276 phosphorylation is a pathway also required for expression of a subset of NF-κB target genes that works in concert with pathways controlling NF-κB translocation. Interestingly, IκBα is NF-κB translocation-dependent gene (41, 42) whose expression, in response to TNF, is independent of phospho-Ser-276 RelA formation. Our finding that RSV-induced IκBα gene expression is not affected by NAC or DMSO treatment suggests that IκBα expression in RSV infection does not require phospho-Ser-276-modified RelA. These data indicate that phospho-Ser-276 controls expression of a subset of the inflammatory NF-κB-dependent genes over a wide range of stimuli.

Investigation of the effects of Ser-to-Ala site mutation at residue 276 indicates that this phosphorylation is required for target gene expression in response to RSV. Ser-276 phosphorylation is an important signaling event in the TNF activation pathway that has multiple effects on protein interaction, posttranslational modifications, and enhanceosome formation (22, 33, 52). Earlier studies have shown that RelA Ser-276 phosphorylation reduces intermolecular NH_2- and COOH-terminal interactions, allowing it to complex with p300/CBP coactivators (50). This posttranslational modification is linked to additional acetylation at Lys-310, an event that stabilizes its association with endogenous gene targets (9). We have also found that RelA Ser-276 phosphorylation allows complex formation with cyclin-dependent kinase 9 (CDK-9)/cyclin T1 (Ccn T1), known as PTEF-b (33). CDK-9/Ccn T1 are involved in phosphorylat-

ing the COOH-terminal domain of RNA polymerase II, licensing polymerase II to produce fully elongated transcripts. The relationship between RelA Ser-276 phosphorylation, acetylation, and complex formation in the context of RSV infection will require further investigation.

MSK1 and the catalytic subunit of PKA, PKAc, are both known to be RelA Ser-276 kinases. Previous work from our group and others has implicated PKAc in mediating TNF-α-inducible RelA Ser-276 phosphorylation (22). However, in data not shown, we have not been able to demonstrate that PKAc plays a role in mediating RSV-inducible phospho-Ser-276 RelA formation. These differences may suggest that distinct NF-κB activating signals utilize MSK1 or PKAc to various degrees. We note, for example, that RSV induces levels of phospho-Ser-376 MSK1 formation similar to those produced by TNF-α, yet its activation profile is longer and more sustained (Fig. 5A). These data may indicate that although MSK1 and PKAc are both ROS-regulated RelA kinases, their involvement in the NF-κB pathway is in a stimulus-dependent manner. We note that MSK1 is known to mediate cytokine expression in psoriatic epidermis (18) and *Helicobacter pylori* infection (35). Our novel finding in this study is that MSK1 is activated by RSV infection via ROS and that it plays a central role in NF-κB activation via RelA Ser-276 phosphorylation.

Our study does not completely address the potential role of other RelA phosphorylation sites and will be a subject for further inquiry. Previous work has shown that RelA Ser-536 phosphorylation occurs on a pool of RelA not associated with IκBα and regulates a distinct subset of NF-κB-dependent genes (37). Moreover, the kinases responsible for Ser-536 phosphorylation are unknown. In this regard, our data indicates that RSV induces phospho-Ser-536 formation in kinetics similar to that of phospho-Ser-276 formation (Fig. 1), but because Ser-536 phosphorylation is controlled by an antioxidant-independent pathway, this indicates that it is independent of MSK1 action. Potential RelA Ser-536 kinases in viral infection include NIK, IKKα/-β/-ε, and others (6, 11, 37). More work will be required to identify the genes controlled by Ser-536 phosphorylation, the kinases responsible for this activation, and the effect of Ser-536 phosphorylation on RelA function.

Identification of pathways controlling NF-κB activation in response to viral infection are likely to have translational applications in the treatment of severe lower respiratory tract infections in humans. Our finding of an ROS-MSK1 pathway provides a mechanism for attenuating the proinflammatory effects of RSV on lung inflammation in lower respiratory tract disease.

ACKNOWLEDGMENTS

This project was supported by NIH grant P01 AI062885 (to A.R.B.) and by NHLBI Proteomics Technologies in Airway Inflammation (grant N01-HV-28184). Core laboratory support was obtained from NIEHS grant P30 ES06676.

REFERENCES

1. **Aggeli, I. K., C. Gaitanaki, and I. Beis.** 2006. Involvement of JNKs and p38-MAPK/MSK1 pathways in H2O2-induced upregulation of heme oxygenase-1 mRNA in H9c2 cells. Cell. Signal. **18:**1801–1812.
2. **Anrather, J., G. Racchumi, and C. Iadecola.** 2005. cis-acting element-specific transcriptional activity of differentially phosphorylated nuclear factor-κB. J. Biol. Chem. **280:**244–252.
3. **Brasier, A. R.** 2006. The NF-κB regulatory network. Cardiovasc. Toxicol. **6:**111–130.
4. **Brasier, A. R.** 2009. The NF-kB signaling network: insights from systems approaches, p. 119–136. *In* A. R. Brasier, S. M. Lemon, and A. Garcia-Sastre (ed.), Cellular signaling and innate immune responses to RNA virus infections. ASM Press, Washington, DC.
5. **Brasier, A. R., P. Liu, and B. Tian.** 2009. Signaling pathways in the host cell response to RSV infection, p. 157–184. *In* D. Yang (ed.), RNA viruses: host gene responses to infections. World Scientific Publishing Co., Hackensack, NJ.
6. **Buss, H., A. Dorrie, M. L. Schmitz, E. Hoffmann, K. Resch, and M. Kracht.** 2004. Constitutive and interleukin-1-inducible phosphorylation of p65 NF-kappaB at serine 536 is mediated by multiple protein kinases including IkappaB kinase (IKK)-alpha, IKKbeta, IKKepsilon, TRAF family member-associated (TANK)-binding kinase 1 (TBK1), and an unknown kinase and couples p65 to TATA-binding protein-associated factor II31-mediated interleukin-8 transcription. J. Biol. Chem. **279:**55633–55643.
7. **Casola, A., N. Burger, T. Liu, M. Jamaluddin, A. R. Brasier, and R. P. Garofalo.** 2001. Oxidant tone regulates RANTES gene expression in airway epithelial cells infected with respiratory syncytial virus. Role in viral-induced interferon regulatory factor activation. J. Biol. Chem. **276:**19715–19722.
8. **Castro, S. M., A. Guerrero-Plata, G. Suarez-Real, P. A. Adegboyega, G. N. Colasurdo, A. M. Khan, R. P. Garofalo, and A. Casola.** 2006. Antioxidant treatment ameliorates respiratory syncytial virus-induced disease and lung inflammation. Am. J. Respir. Crit. Care Med. **174:**1361–1369.
9. **Chen, L.-F., W. Fischel, E. Verdin, and W. C. Greene.** 2001. Duration of nuclear NF-kB action regulated by reversible acetylation. Science **293:**1653–1657.
10. **Chen, L. F., S. A. Williams, Y. Mu, H. Nakano, J. M. Duerr, L. Buckbinder, and W. C. Greene.** 2005. NF-κB RelA phosphorylation regulates RelA acetylation. Mol. Cell. Biol. **25:**7966–7975.
11. **Choudhary, S., M. Lu, R. Cui, and A. R. Brasier.** 2007. Involvement of a novel Rac/RhoA GTPase-NF-κB inducing kinase (NIK) signaling pathway mediating angiotensin II-induced RelA transactivation. Mol. Endocrinol. **21:**2203–2217.
12. **Collins, P. L., and G. W. Wertz.** 1983. cDNA cloning and transcriptional mapping of nine polyadenylated RNAs encoded by the genome of human respiratory syncytial virus. Proc. Natl. Acad. Sci. USA **80:**3208–3212.
13. **Cui, R., B. Tieu, A. I. Recinos, R. G. Tilton, and A. R. Brasier.** 2006. Rho A mediates angiotensin II-induced phospho-Ser536 NF-kB/RelA subunit exchange on the IL-6 promoter in VSMC. Circ. Res. **99:**723–730.
14. **Dong, C., R. J. Davis, and R. A. Flavell.** 2002. MAP kinases in the immune response. Annu. Rev. Immunol. **20:**55–72.
15. **Ea, C. K., L. Deng, Z. P. Xia, G. Pineda, and Z. J. Chen.** 2006. Activation of IKK by TNFalpha requires site-specific ubiquitination of RIP1 and polyubiquitin binding by NEMO. Mol. Cell **22:**245–257.
16. **Forbus, J., H. Spratt, J. Wiktorowicz, Z. Wu, I. Boldogh, L. Denner, A. Kurosky, R. C. Brasier, B. Luxon, and A. R. Brasier.** 2006. Functional analysis of the nuclear proteome of human A549 alveolar epithelial cells by HPLC-high resolution 2D gel electrophoresis. Proteomics **6:**2656–2672.
17. **Foster, K. A., C. G. Oster, M. M. Mayer, M. L. Avery, and K. L. Audus.** 1998. Characterization of the A549 cell line as a type II pulmonary epithelial cell model for drug metabolism. Exp. Cell Res. **243:**359–366.
18. **Funding, A. T., C. Johansen, K. Kragballe, K. Otkjaer, U. B. Jensen, M. W. Madsen, M. S. Fjording, J. Finnemann, T. Skak-Nielsen, S. R. Paludan, and L. Iversen.** 2006. Mitogen- and stress-activated protein kinase 1 is activated in lesional psoriatic epidermis and regulates the expression of pro-inflammatory cytokines. J. Investig. Dermatol. **126:**1784–1791.
19. **Garofalo, R., M. Sabry, M. Jamaluddin, R. K. Yu, A. Casola, P. L. Ogra, and A. R. Brasier.** 1996. Transcriptional activation of the interleukin-8 gene by RSV infection in alveolar epithelial cells: nuclear translocation of the RelA transcription factor as a mechanism producing airway mucosal inflammation. J. Virol. **70:**8773–8781.
20. **Haeberle, H., R. Takizawa, A. Casola, A. R. Brasier, H.-J. Dieterich, N. van Rooijen, Z. Gatalica, and R. P. Garofalo.** 2002. Respiratory syncytial virus-induced activation of NF-kB in the lung involves alveolar macrophages and toll-like receptor 4-dependent pathways. J. Infect. Dis. **186:**1199–1206.
21. **Hall, C. B.** 2001. Respiratory syncytial virus and parainfluenza virus. N. Engl. J. Med. **344:**1917–1928.
22. **Jamaluddin, M., S. Wang, I. Boldogh, B. Tian, and A. R. Brasier.** 2007. TNF-α-induced NF-κB/RelA Ser 276 phosphorylation and enhanceosome formation on the IL-8 promoter is mediated by a reactive oxygen species (ROS)-dependent pathway. Cell. Signal. **9:**1419–1433.
23. **Jamaluddin, M., A. Casola, R. P. Garofalo, Y. Han, T. Elliott, P. L. Ogra, and A. R. Brasier.** 1998. The major component of IkBa proteolysis occurs independently of the proteasome pathway in respiratory syncytial virus-infected pulmonary epithelial cells. J. Virol. **72:**4849–4857.
24. **Jamaluddin, M., S. Wang, R. Garofalo, T. Elliott, A. Casola, S. Baron, and A. R. Brasier.** 2001. IFNb mediates coordinate expression of antigen-processing genes in RSV infected pulmonary epithelial cells. Am. J. Physiol. Lung Cell. Mol. Physiol. **280:**L248–L257.
25. **Jewell, N. A., N. Vaghefi, S. E. Mertz, P. Akter, R. S. Peebles, Jr., L. O. Bakaletz, R. K. Durbin, E. Flano, and J. E. Durbin.** 2007. Differential type I interferon induction by respiratory syncytial virus and influenza A virus in vivo. J. Virol. **81:**9790–9800.

26. **Lamothe, B., A. Besse, A. D. Campos, W. K. Webster, H. Wu, and B. G. Darnay.** 2007. Site-specific Lys-63-linked tumor necrosis factor receptor-associated factor 6 auto-ubiquitination is a critical determinant of IkappaB kinase activation. J. Biol. Chem. **282:**4102–4112.
27. **Lin, R., L. Yang, P. Nakhaei, Q. Sun, E. Sharif-Askari, I. Julkunen, and J. Hiscott.** 2006. Negative regulation of the retinoic acid-inducible gene I-induced antiviral state by the ubiquitin-editing protein A20. J. Biol. Chem. **281:**2095–2103.
28. **Liu, P., M. Jamaluddin, K. Li, R. P. Garofalo, A. Casola, and A. R. Brasier.** 2007. Retinoic acid-inducible gene I mediates early antiviral response and Toll-like receptor 3 expression in respiratory syncytial virus-infected airway epithelial cells. J. Virol. **81:**1401–1411.
29. **Liu, P., K. Li, R. P. Garofalo, and A. R. Brasier.** 2008. RSV induces RelA release from cytoplasmic 100 kDa NF-κB2 complexes via a novel retinoic acid inducible gene-I-NF-κB inducing kinase (NIK) signaling pathway. J. Biol. Chem. **283:**23169–23178.
30. **Liu, T., S. Castro, A. R. Brasier, M. Jamaluddin, R. P. Garofalo, and A. Casola.** 2004. Reactive oxygen species mediate virus-induced STAT activation: role of tyrosine phosphatases. J. Biol. Chem. **279:**2461–2469.
31. **MacDonald, N. E., C. B. Hall, and S. C. Suffin.** 1982. Respiratory syncytial viral infection in infants with congenital heart disease. N. Engl. J. Med. **307:**397–400.
32. **McCoy, C. E., D. G. Campbell, M. Deak, G. B. Bloomberg, and J. S. Arthur.** 2005. MSK1 activity is controlled by multiple phosphorylation sites. Biochem. J. **387:**507–517.
33. **Nowak, D. E., B. Tian, M. Jamaluddin, I. Boldogh, L. A. Vergara, S. Choudhary, and A. R. Brasier.** 2008. RelA Ser276 phosphorylation is required for activation of a subset of NF-κB-dependent genes by recruiting cyclin-dependent kinase 9/cyclin T1 complexes. Mol. Cell. Biol. **28:**3623–3638.
34. **Oshiumi, H., M. Matsumoto, S. Hatakeyama, and T. Seya.** 2009. Riplet/RNF135, a RING finger protein, ubiquitinates RIG-I to promote interferon-beta induction during the early phase of viral infection. J. Biol. Chem. **284:**807–817.
35. **Pathak, S. K., S. Basu, A. Bhattacharyya, S. Pathak, A. Banerjee, J. Basu, and M. Kundu.** 2006. TLR4-dependent NF-kappaB activation and mitogen- and stress-activated protein kinase 1-triggered phosphorylation events are central to Helicobacter pylori peptidyl prolyl cis-, trans-isomerase (HP0175)-mediated induction of IL-6 release from macrophages. J. Immunol. **177:**7950–7958.
36. **Peterhans, H., M. Grob, T. Burge, and R. Zanoni.** 1987. Virus-induced formation of reactive oxygen intermediates in phagocytic cells. Free Radic. Res. Commun. **3:**39–46.
37. **Sasaki, C. Y., T. J. Barberi, P. Ghosh, and D. L. Longo.** 2005. Phosphorylation of RelA/p65 on serine 536 defines an IkappaBalpha-independent NF-kappaB pathway. J. Biol. Chem. **280:**34538–34547.
38. **Schwarz, K. B.** 1996. Oxidative stress during viral infection: a review. Free Radic. Biol. Med. **21:**641–649.
39. **Shembade, N., N. S. Harhaj, K. Parvatiyar, N. G. Copeland, N. A. Jenkins, L. E. Matesic, and E. W. Harhaj.** 2008. The E3 ligase Itch negatively regulates inflammatory signaling pathways by controlling the function of the ubiquitin-editing enzyme A20. Nat. Immunol. **9:**254–262.
40. **Shembade, N., K. Parvatiyar, N. S. Harhaj, and E. W. Harhaj.** 2009. The ubiquitin-editing enzyme A20 requires RNF11 to downregulate NF-κB signalling. EMBO J. **28:**513–522.
41. **Tian, B., D. Nowak, and A. R. Brasier.** 2005. A TNF induced gene expression program under oscillatory NF-κB control. BMC Genomics **6:**137.
42. **Tian, B., Y. Zhang, B. A. Luxon, R. P. Garofalo, A. Casola, M. Sinha, and A. R. Brasier.** 2002. Identification of NF-κB-dependent gene networks in respiratory syncytial virus-infected cells. J. Virol. **76:**6800–6814.
43. **Vermeulen, L., G. De Wilde, P. Van Damme, W. Vanden Berghe, and G. Haegeman.** 2003. Transcriptional activation of the NF-kappaB p65 subunit by mitogen- and stress-activated protein kinase-1 (MSK1). EMBO J. **22:**1313–1324.
44. **Vlahopoulos, S., I. Boldogh, and A. R. Brasier.** 1999. NF-κB dependent induction of interleukin-8 gene expression by tumor necrosis factor α: evidence for an antioxidant sensitive activating pathway distinct from nuclear translocation. Blood **94:**1878–1889.
45. **Wang, D., S. D. Westerheide, J. L. Hanson, and A. S. J. Baldwin.** 2000. TNFalpha-induced phosphorylation of RelA/p65 on Ser529 is controlled by casein kinase II. J. Biol. Chem. **275:**32592–32597.
46. **Welliver, T. P., R. P. Garofalo, Y. Hosakote, K. H. Hintz, L. Avendano, K. Sanchez, L. Velozo, H. Jafri, S. Chavez-Bueno, P. L. Ogra, L. McKinney, J. L. Reed, and R. C. Welliver, Sr.** 2007. Severe human lower respiratory tract illness caused by respiratory syncytial virus and influenza virus is characterized by the absence of pulmonary cytotoxic lymphocyte responses. J. Infect. Dis. **195:**1126–1136.
47. **Wiggin, G. R., A. Soloaga, J. M. Foster, V. Murray-Tait, P. Cohen, and J. S. Arthur.** 2002. MSK1 and MSK2 are required for the mitogen- and stress-induced phosphorylation of CREB and ATF1 in fibroblasts. Mol. Cell. Biol. **22:**2871–2881.
48. **Wu, C. J., D. B. Conze, T. Li, S. M. Srinivasula, and J. D. Ashwell.** 2006. Sensing of Lys 63-linked polyubiquitination by NEMO is a key event in NF-κB activation. Nat. Cell Biol. **8:**398–406.
49. **Zhang, Y., B. A. Luxon, A. Casola, R. P. Garofalo, M. Jamaluddin, and A. R. Brasier.** 2001. Expression of RSV-induced chemokine gene networks in lower airway epithelial cells revealed by cDNA microarrays. J. Virol. **75:**9044–9058.
50. **Zhong, H., H. SuYahng, H. Erdjument-Bromage, P. Tempst, and S. Ghosh.** 1997. The transcriptional activity of NF-kB is regulated by the IkB-associated PKAc subunit through a cyclic AMP-independent mechanism. Cell **89:**413–424.
51. **Zhong, H., R. E. Voll, and S. Ghosh.** 1998. Phosphorylation of NF-kB p65 by PKA stimulates transcriptional activity by promoting a novel bivalent interaction with the coactivator CBP/p300. Mol. Cell **1:**661–671.
52. **Zhong, H., M. J. May, E. Jimi, and S. Ghosh.** 2002. The phosphorylation status of nuclear NF-κB determines its association with CBP/p300 or HDAC-1. Mol. Cell **9:**625–636.